13th Conference on Nuclear and Particle Physics

NUPPAC' 24



23-26 September 2024
Marsa Matrouh, Egypt

NUPPAC' 24

Conference Scientific Sessions

Monday, 23 Sep 2024

15:30 - 17:00	Conference Opening
	Oral-1

Tuesday, 24 Sep 2024

9:00 - 10:15	Session Oral-2
10:15 - 11:00	Session PKN-1
11:00 - 12:00	Session Oral-3
12:00 - 13:30	Session PKN-2
14:15 - 15:30	Session Oral-4
15:30 - 17:00	Session PS

Thursday, 25 Sep 2024

9:00 - 10:00	Oral-5
10:00 - 10:45	PKN-3
10:45 – 11:00	Conference Closing

NUPPAC' 24

Conference Timetable

Time	Mon., 23 Sep	Time	Tue., 24 Sep.	Wed., 25 Sep.	Time	Thu., 26 Sep.
7:00-7:45	Gathering Pre-Registration	8:00-9:00	Breakfast	Breakfast	8:00-9:00	Breakfast
8:00	**Departure Cairo**	9:00-10:15	**Oral-2**	**Full**	9:00-10:00	**Oral-5**
10:30-11:00	Mid-way Rest	10:15-11:00	**PKN-1**	**Day**	10:00-10:45	**PKN-3**
		11:00-12:00	**Oral-3**		10:45-11:30	**CS** Tea/Cofee
14:00-14:30	**Arrival Marsa**	12:00-13:30	**PKN-2**	**Marsa**	11:30-12:00	Hotel Check- Out
14:30	Hotel Check-In	13:30-14:15	Tea/Cofee	**Matrouh**	12:30	**Departure to Cairo**
15:00-15:30	Tea/Cofee Conf Regist	14:15-15:30	**Oral-4**	**and**	15:30-16:00	Mid-way Rest
15:30-17:00	**OS/ Oral-1**	15:30-17:00	**Poster**	**Attractions**		
19:00-20:00	Dinner	19:00-21:00	Dinner	Dinner	19:00-19:30	**Arrival Cairo**
20:00-22:00	Free Evening	21:00-23:00	Cult Evening	Free Evening		

Programme abbreviations

OS	Opening Session	**Oral**	Oral Session
IKN	Plenary/Keynote Talks	**CS**	Closing Session

NUPPAC' 24

Conference Abstracts Arranged by Receiving Date

(Numbered according to the list of abstracts on the conference web site)

1.

Temperature effect on nuclear statistical quantities in the isovector plus isoscalar neutron-proton pairing case *(P1)*

D. Mokhtari , N.H. Allal and M. Fellah

USTHB BP 32, El-Alia, 16111 Bab-Ezzouar, Algiers, Algeria.

Due to fast progress in Radioactive Ion Beam programs, the study of neutron-proton (n-p) pairing effects has known a renewal of interest during the last decade (cf. e.g. [1-3]). N-p pairing effects may exist in two forms: the isovector (T=1) and the isoscalar (T=0) pairing, where T is the isospin quantum number. On the other hand, the study of the temperature effect on pairing correlations at finite temperature have been the subject of many efforts since the sixties and is still a relevant subject [3- 5]. In the present work, expressions of the various statistical quantities, i. e. , the energy, the entropy and the heat capacity are established using a path integral approach in the T=1 plus T=0 n-p pairing case [6]. A numerical study is then performed using the schematic one level model. It's shown that the inclusion of the isoscalar pairing in addition to the isovector one leads to a lowering of the energy as well as a change of the shapes of energy, entropy and heat capacity curves as a function of the temperature.

References:

1. D. Negrea, N. Sandulescu and D. Gambacurta, Phys. Rev. C105 (2022) 034325.

2. D. Mokhtari, M. Fellah and N.H. Allal, Int. J. Mod. Phys. E 25 (2016) 1650035.
3. M. Fellah, N.H. Allal, M. Belabbas, M.R. Oudih and N. Benhamouda, Phys. Rev. C 76 (2007) 047306.
4. A.L. Goodman, Nucl Phys. A402 (1983) 189.
5. K. Kaneko and M. Hasegawa, Phys. Rev. C 72 (2005) 031302(R).
6. D. Mokhtari, N.H. Allal and M. Fellah, Int. J. Mod. Phys. E 27 (2018) 1850054. `
.

2-

Nuclear equation of state from nuclear structure to neutron stars *(O1)*

Walaa M. Seif,
Cairo University, Faculty of Science, Department of Physics, 12613 Giza, Egypt
Joint Institute for Nuclear Research, 141980 Dubna, Russia
The Academy of Scientific Research and Technology, 4262104 Cairo, Egypt
wseif@sci.cu.edu.eg

The equation of state of asymmetric nuclear matter and its isospin-asymmetry dependence influence most of the nuclear structure, reactions, and decays, in addition to the structure of neutron stars and their formation. Towards a well-defined nuclear equation of state, it is crucial to investigate a wide range of nuclear and astrophysical systems under extreme low and high nuclear density and pressure. A correct equation of state would help in understanding ground-state structure properties of finite nuclei, the stability of neutron-rich and superheavy nuclei, heavy-ion collision dynamics, giant monopole resonance and excitation energies, and the surface energy and surface diffuseness of nuclei, as well as the neutron star structure. The masses, radii, and tidal deformability of neutron stars that extracted from astrophysical data can be used

to probe the equation of state of dense nuclear matter, up to a few times the nuclear saturation density.

3-

Eigen solution of rovibrational bound state of the energy dependent general molecular potential in the case of diatomic molecules *(P2)*

R. Yekken[a], A. Haddouche[a,b] and S. Boufas[a]
[a]Laboratoire de Physique Théorique et de didactique, Faculté de Physique, Université des Sciences et de la Technologie Houari Boumediene, USTHB. BP 32, Al-Alia, 16111, Bab Ezzouar, Alger, Algeria.
[b]Département des classes préparatoires, Ecole Nationale Supérieure des Travaux Publics, BP 32 Rue Sidi Garidi, 16006, Kouba, Alger, Algeria

Particular attention was paid to the treatment of a class of Hamiltonians whose interaction potential is energy dependent. The interest in this kind of potentials is motivated by the fact that they present a way to include nonlinear effects in the Schrödinger equation. Such quantum situations arise from the relativistic nature of the studied systems.

In this work, we are focused on the analytical calculation of the energy spectrum linked to rovibrational bound states of the energy dependent general molecular potential (EDGMP). Within the framework of non-relativistic quantum mechanics, the treatment of the three dimensional wave equation for any arbitrary angular momentum$(\ell \neq 0)$, becomes possible by using the Pekeris approximation of the centrifugal term. The analytical solutions of the result equation with the alternative form of the effective potential are obtained by the asymptotic iteration method (AIM). The energy spectrum expression is obtained as well as the corresponding normalized

eigenfunctions are derived in terms of generalized hypergeometric functions. As applications, we are studied for finite electronic states some diatomic molecules

4-

Thorium reactors and the future of nuclear power *(O2)*

M.N.H. Comsan,

Egyptian Nuclear Physics Association, Cairo, Egypt

The raising problem of fossil fuel reserve limitation along with environmental constrains connected with the climate change and necessity to reduce CO_2 emissions led to the recognition of nuclear energy as green energy. Currently nuclear energy amounts for ~10% of the global generating electricity of ~4300 GW. Of the three known nuclear fuel elements: thorium, uranium and plutonium, most of the operating nuclear reactors use uranium or a mix of uranium-plutonium as their fuel. As a result of using of such a fuel for more than 50 years, a huge amount of long lived hazardous radioactive waste has been accumulated.

On the other hand, thorium as nuclear material has several advantages over uranium. Among others, the advantages include favorable nuclear properties, along with a much reduced nuclear waste.

An overview is given of thorium as a prospective natural source for future energy, its world resources (including in Egypt), the rational of thorium-based fuel cycle, reasons behind the selection of thorium fuel, issues to be considered while dealing with thorium nuclear fuel cycle, thorium utilization in experimental and power reactors in countries such as India, Germany, the UK, France, Japan, Russia, Canada, Brazil, and China.

5-

Isotopic effects in the He^+ - He collision at lower energies *(O3)*

F. Bouchelaghem, S. Lias, S. Nehaoua, A. Ghezal

^{1,3,4}Physics Department, Mohamed Boudiaf University, University Pole, Road Bourdj Bou Arreiridj, M'sila 28000.

^{2}Algeria University of Science and Technology Houari Boumediene BP 32 Bab Ezzouar, 16111. Algeria

This work is devoted to calculating the potential-energy curves of helium ions in their gases such as $He^+(2s)$- He(1s), when both species are in their ground states, are either gerade (g) or ungerade (u), namely, Σ_{g}^{+} or Σ_{u}^{+} in the field of energy 10^{-} $\leq E \leq 10^{-}$(a.u.), using new and modern data. Elastic cross-sections have also been calculated and the isotope effect of the presence of ^{4}He and ^{3}He atoms has been addressed, taking into account the nuclear spin and analog effect emanating from similar and non-distinction between colliding atoms*)*

6-

Novel quantum mechanics in the multi-component glasses *(O4)*

Giancarlo Jug

INFN (Istituto Nazionale di Fisica Nucleare), Sezione di Pavia (Italy)

and DiSAT, Università dell'Insubria, Como (Italy)

Glasses are fascinating substances, attractive for both the arts and for technical applications since Ancient Egyptian times. Here I will talk about their physical properties on fundamental grounds.

It is well known that the physically-detectable particles of physics are charged only in terms of the electron's charge e, the

exception being quarks (with e/3, 2e/3) that however remain tightly bound. In condensed matter, as in the case of a two-dimensional Coulomb gas, there are however elementary collective EXCITATIONS above the ground state that can display an effective charge that is a rational fraction 1/3, 1/5, 1/7 etc. of e (as in the Fractional Quantum Hall Effect) and manifest themselves in the plateaus of the electric Hall conductivity vs the magnetic field.

I will argue that in the insulating glasses taken at low temperatures there are elementary excitations of strongly-interacting charged mobile species tunneling in the pockets (of typical nano-metric size) of the glassy structure and which can take up fractions of e of arbitrary values in terms of the effective electric charge. These fractions are determined by the size of such voids and manifest themselves in terms of the intrinsic magnetization of glasses and other magnetic effects. Such arbitrary fractional electric charges can be detected indirectly through low-temperature magnetization measurements and are collective violations of the fundamental quantization of the electric charge in Nature.

7-

Theoretical formulae of (n,^{3}He) reaction function excitation at 14,6 MeV *(P3)*

Samra Nehaoua, Fouzia Bouchelaghem, Asma Ghezal, Nouri Benaidja

Uuniversity of Msila, Algeria

A new three parameters formulae for (n,^{3}He) nuclear reaction is proposed to calculate function excitation at 14.6 MeV, this semi-empirical systematic reduces parameters taken in previous proposed formulae which increase the contribution of pre-equilibrium 3He particle emission. We use exciton

model in closed form and coalescence model to describe the pre-equilibrium 3He particle emission in reaction induced by neutron. To check the formula's quality we compare obtained cross section with measured ones. The formula obtained in this work has a good fitting with lower values of statistical parameters.

8-

New semi empirical systematic of (n,t) reaction cross section *(P4)*

Asma Ghezal, Samra Nehaoua, Fouzia Bouchelaghem

Laboratory of materials and renewable energy, faculty of science Department of physics, university of Msila, PO Box 166 Ichebilia 28000 M'sila, Algeria

A semi-empirical formula for the (n,t) nuclear reaction is used to calculate the excitation function at 14.6 MeV. This semi-empirical systematic, with three parameters fixed by experimental data, uses theoretical models to describe tritium emission in neutron reactions. To verify the quality of the proposed formula, we compare the obtained cross-section with measured ones. The calculated (n, t) excitation function is close to the experimental excitation function. The formula obtained in this work better describes tritium emission.

9-

Thermophysical properties of helium and argon gas *(O5)*

Fouzia Bouchelaghem, Moncef Chicouche, Hayette Boutarfa, Samra Nehaoua

Physics Department, Mohamed Boudiaf University,M'sila, 28000, Algeria.

In this work, the thermophysical properties of a helium

and argon dilute gas are revisited, in the range of low and high temperatures, with new and recent potential data points. The calculations of various transport parameters, namely diffusion, viscosity, and thermal conductivity, are extended to include the nuclear spins and the symmetry effects, which arise from the identity and indistinguishability of the colliding atoms. The results, mainly at high temperatures for ^{4}He, are in a good agreement with the published values but for ^{39}Ar at high and base temperatures are in a good agreement with the published values.

.

10-

New formula for charge-change cross section of nucleus-nucleus interaction *(O6)*

I.A.M. Abdulmagead

Physics Department - Faculty of Science – Cairo University - Giza 12613 - Egypt

By including the projectile neutron contribution, we developed a free parameter formula based on the Glauber model framework for nucleus-nucleus interaction to determine the total charge change cross section σcc. The formula successfully reproduced the experimental data of reactions ^{9}Be+^{12}C, ^{16,17}O+^{12}C, ^{27}Al+^{12}C, ^{28}Si+^{12}C, ^{40}Ar+^{12}C, ^{56}Fe+^{12}C, and ^{238}U+^{12}C. Consequently, our study ensures that the charge change cross sections depend on the projectile's neutrons, as well as its protons.

Keywords: charge change cross section, Glauber model, neutron contribution

11-

Analysis of proton-nucleus scattering data at energies 200-1000 MeV within the microscopic model of folding optical potential *(O7)*

Elena Zemlyanaya, Valery Lukyanov, Konstantin Lukyanov, Ibrahim Abdul-Magead

Joint Institute for Nuclear Research, Dubna, Russia

The cross sections of proton-nucleus elastic and inelastic scattering at energies from 200 to 1000 MeV are calculated within the microscopic model of folding optical potential. Such potential is determined by the density of target nucleus and on the amplitude of scattering of incident proton on the bound nuclear nucleon. The amplitude itself depends on three parameters, namely the total nucleon-nucleon scattering cross section, the ratio of real to imaginary parts of the scattering amplitude at forward angles, and the slope parameter. These "inmedium" scattering amplitude parameters are adjusted to the experimental data on elastic proton-nucleus scattering. The "inmedium" parameters are compared with the "free" ones known from analysis of proton-nucleon scattering data. Such analysis allows one to estimate effect on nuclear matter on the scattering amplitude.

12-

Properties of heavy nuclei by laser spectroscopy methods *(O8)*

S. Zemlyanoy, A. Rodin, G. Myshinski, B. Zhemenik *Joint Institute for Nuclear Research, Dubna 141980, Russia*, **Yu. Kudryavtsev** *Instituut voor Kern- en Stralingsfysica, Leuven, Belgium,* **V. Fedosseev** *CERN, Switzerland*, **R. Bark** *iThemba LABS, Nat. Research Foundation, South Africa*

E-mail: *zemlya@jinr.ru*

A new setup, based on stopping nuclei in the gas cell and subsequent resonance laser ionization and separation by magnetic field or time of flight is under stage of realization at JINR Flerov Lab. This setup is devoted to synthesis and study of new heavy nuclei formed in low energy multi-nucleon transfer or fusion reactions. The heavy nuclei are very important for nuclear physics investigations, for the understanding of fusion – evaporation processes, stability of heavy nuclei, limits of existence of heavy and superheavy nuclei, astrophysical nucleosynthesis and r-process. The properties of heavy nuclei, as nuclear shape and size is a key point in constructing of nuclear models and predictions of properties of new nuclei. Ionization potentials and mobility of atoms and ions of heavy elements are extremely important in understanding their chemical properties and role of relativistic effects. A creation and launch of this facility will open a new field of research in low-energy heavy-ion physics, and new horizons in the study of unexplored "north-east" area of the nuclear map. It could be helpful also for finding a new way for production of heavy and superheavy nuclei and investigation of their properties.

13-

Synthesis of ternary semiconductor GaPAl by fast ion implantation and its identification analysis by laser Raman spectroscopy *(O9)*

Sergo V. Gotoshia

Ivane Javakhishvili Tbilisi State University, R. Agladze Institute of Inorganic Chemistry and Electrochemistry, Laser Center, Georgia, 0186, Tbilisi, Mindeli Street 11

srgotoshia@yahoo.com

As it is known, different types of radiation defects are formed during the implantation of fast ions in the semiconductor layer. When implanted in large doses, an amorphous ternary compound may form near the surface. A ternary compound can potentially be synthesized by implanting the layer with ions that cause replacement of the main lattice ions in the semiconductor. We bombarded the gallium phosphide surface with aluminum ions. Aluminum in the lattice should replace gallium and form a ternary solid solution GaPAl.

We implanted the 001 orientation surface of monocrystalline gallium phosphide with 60 and 100 keV aluminum ions. The flow of ions in the first case was 8.7×10^{16} ions/cm^2, and in the second case it was 2.8×10^{16} ions/cm^2. We performed implantation at a temperature of 400^0C. The projected range R_p of aluminum in gallium phosphide is 49.1 nm and struggle DR_p is 35.8 nm at 60 keV. The projected range R_p of aluminum in gallium phosphide is 85 nm and struggle DR_p is 54 nm at 100 keV. Therefore, the synthesized ternary amorphous solid solution, GaPAl, must be synthesized at different depths from the surface. The thickness of the synthesized thin layer will also be different.

Identification and analysis of the compound synthesized by ion implantation was carried out using laser Raman spectroscopy. We used a laser Raman system constructed by us to register Raman spectra. This system was built on the basis of the DFS-24 double spectrometer with high resolution. The focal length of the spectrometer was 800 mm, and the resolution was 1 cm^{-1}. We used argon laser wavelength of 514.5 nm to excite Raman spectra. All spectra were recorded at room temperature.

Fig. 1 shows the Raman spectrum of GaPAl, an amorphous ternary semiconductor synthesized by ion implantation, which

we recorded at room temperature using an excitation argon laser wavelength of 514.5 nm. The spectra were recorded when

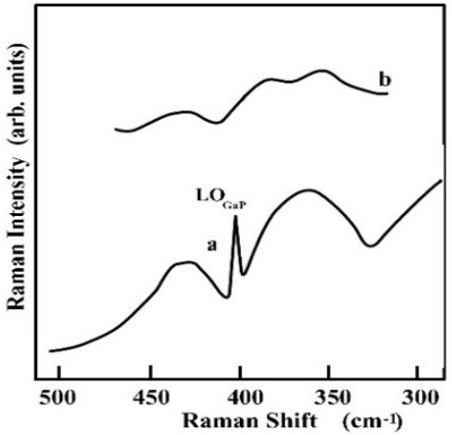


Fig. 1 Raman spectra of α-$Ga_xAl_{1-x}P$ synthesized by Al^+ implantation with two different energies: 60 keV (1a) and 100 keV (1b); exitation λ_L=514.5 nm

aluminum ions were implanted at two different energies. As mentioned above, a new amorphous ternary compound GaPAl is formed at different depths. This picture is clearly expressed in Fig. 1 given Raman spectra. Two broad bands are visible in the spectra. From this, the low-frequency band reflects the characteristic phonon oscillations of the gallium phosphide sublattice of the ternary compound. The wide high-frequency band corresponds to the phonon oscillations of the aluminum phosphide sublattice of the ternary amorphous compound. The phonon oscillations of amorphous gallium phosphide itself are characterized by one broad band, the structure of which is less pronounced. This is shown in Fig. 2b. Figure 2a shows the LO and TO phonons of crystalline gallium phosphide. It is clearly seen that the characteristic broad band of the amorphous phase is shifted to lower frequencies from the phonons of the crystalline phase. Furthermore, by comparing the spectra, it can be seen that the characteristic broad band of the ternary

amorphous phase, which represents the gallium phosphide sublattice oscillations, is displaced from the individual amorphous gallium phosphide spectral band.

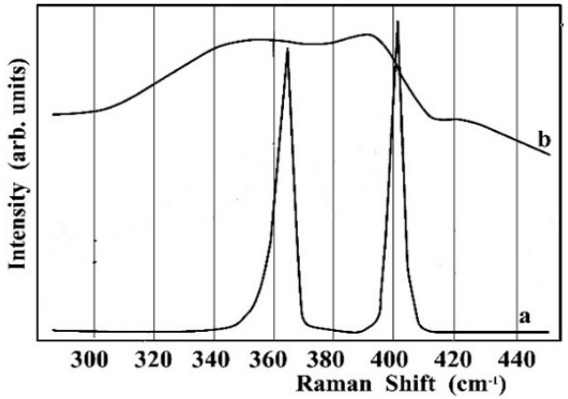


Fig. 2 Raman spectrum of crystalline gallium phosphide of a-111 orientation;Amorphous gallium phosphide synthesized by b-ion implantation.

In addition, there is the formation of an extra high frequency wide band. This band characterizes the oscillations of the aluminum phosphide sublattice and unambiguously confirms the formation of the single-phase amorphous ternary semiconductor GaPAl.

Spectral bands characteristic of phonon oscillation in amorphous systems are broad and unstructured. The reason for this is that in amorphous solids, the crystal long-range order, periodicity is lost. Therefore, all phonons are active here, and therefore Raman spectra literally reflect the state of phonon density. With the corresponding formula, we calculated the state of phonon density curve of the synthesized ternary compound GaPAl.

Thus, using Raman spectroscopy, we have unambiguously established that by ion implantation, in particular by implantation of aluminum in gallium phosphide, it is possible to synthesize the ternary semiconductor GaPAl in the amorphous phase.

14-

Dose calculations and determination of shielding characteristics for protecting emergency workers during the response to radiological emergencies *O(10)*

Wafaa F. Bakr, Noha Shaaban and Nawal M. Said

Regulations and Nuclear Emergencies Division- Nuclear and Radiological Safety Research Center, EAEA, Cairo, Egypt

Effective and efficient response to radiation emergency including those with security related events is the main goal of the national strategy for Emergency preparedness and response. Accidents due to radioactive sources have a wide range of possibilities and consequences. Mapping of the radiation doses related to the exposure of radioactive sources with different activities give a fast view and expectation of the consequences and the required protective actions and other response actions. The aim of this publication is to provide practical guidance, for emergency response in terms of absorbed dose rate and their related required shielding parameters for different category of radioactive source that, if implemented, will provide a fast assessment and response capability needed to protect the public and the workers in the event of different types of radiological emergencies including radioactive sources. MNCP Code is used for predicting the absorbed doses from the famous radioactive sources under different hazard categories (categories 2&3) in case of loss of their shielding at different distances and to calculate their appropriate shielding characteristics.

15-

Impact of replacement coal and fossil energy by nuclear energy on global greenhouse gases emission *(P5)*

Mohamed Abdelaziz[1], Hesham Elkhatib[2*], Abdelfatah Abdelmaksoud[2], Mohamed Essawy[2]

[1]Department of Nuclear Safety Research and Radiological Emergencies, Egyptian Atomic Energy Authority

[2]Nuclear Reactors Department, Egyptian Atomic Energy Authority

Climate change has become one of the important matters that worry humanity worldwide, until local seminars and international conferences have been held for it at the highest levels, such as the level of heads of state. What is worrying about climate change is the increase in the average global temperature until it soon reaches the age of mankind, which has reached 1.5 degrees Celsius until the year 2033 and 2 degrees Celsius until the year 2059, as an inevitable result of the increase in carbon emissions resulting from electricity generation, industry and vehicle exhaust, which were estimated at about 1000 gigabytes of tons until the year 2060, in which the production of electrical energy contributes by more than 50%. On the other hand, the unjust encroachment on forests, this is the lung of the world. Since electric power generation is responsible for more than half of the global emissions of carbon gases, this research aims to study the carbon emissions resulting from electric power generation with the scenarios of Unfinished Symphony, Modern Jazz and Hard Rock, and trying to reduce the carbon emissions resulting from electric power generation by replacing electricity generation with nuclear energy as an alternative to coal all types, as well as petroleum (fossil fuels), with the stability of the use of natural gas and new and renewable energies according to previous scenarios

until the year 2060. The result was, according to the Unfinished Symphony scenario, emissions were about (591.9) Giga tons. In contrast, when using nuclear energy as an alternative, the contribution of electricity production by 65% cancels out the improvement in the amount of carbon emissions by 75.1%, with a carbon dioxide productivity of 146.8 Giga tons. According to the Jazz scenario, emissions were about (632.1) Giga tons. In contrast, when using nuclear energy as an alternative, the contribution of electricity production is 65%, which cancels out the improvement in the amount of carbon emissions by 75.2%, with a carbon dioxide productivity of 156.8 Giga tons. According to the Hard Rock scenario, emissions were about (643.3) Giga tons. In contrast, when using nuclear energy as an alternative, the contribution of electricity production is 65%, which cancels out the improvement in the amount of carbon emissions by 74.87%, with a production of carbon dioxide that amounted to 161.6 Giga tons.

Keywords: Climate change – Co_2 emission – Electric demand scenario – Nuclear energy contribution.

16-

Fabrication of Nano Scintillation Detectors *(O11)*

Amer Mahmoud Amer Hassan

1-Laboratory of Nuclear Problems, JINR, 141980, Dubna, Moscow region, Russia, and

2-Reactor Physics Department, Nuclear Research Center, Egyptian Atomic Energy Authority, P.O. Box 13759, Cairo, Egypt

Nano organic molecules have attracted much of my interest to fabricate novel functional devices. Interfaces between organic semiconductors have crucial roles in

determining the electronic properties of devices ranging from field-effect transistors (FETs) to photovoltaics and scintillations, which is a flash of light produced in a transparent material by an ionization event; the process of scintillation is one of luminescence whereby light of a characteristic spectrum is emitted following the absorption of radiation. Interface and fabrication an ultrathin film play important roles in the scintillation efficiency, this condition has been achieved in my study by depositing 4,4��diamino-p-terphenyl (DAT Figure 1(a)) on the Si (001), DAT is a good candidate for a silicon substrate. DAT has been employed for electroluminescence (EL) devices prepared by vapor deposition polymerization. So, the thicknesses of devices using DAT can be easily controlled at molecular level in the vapor polymerization process. Organic composite scintillators such as p-terphenyl can be compared with the organic liquid scintillators, composites are solids and less flammable; flash point for p-terphenyl is 207 ^{o}C and for stilbene over than 112 ^{o}C. Composite scintillators are sensitive not only to fast neutrons, but also to ɣ-rays; however, the signals from these events can be well separated. The composite scintillators can also be obtained in larger diameter than organic single crystals, but they must be thin enough to achieve the performance which is the key of issue. A simplified diagram of the setup shown in Figure 2., samples attached to photomultiplier tube PMT, the pulse shape discrimination (PSD) performed by means of a zero−crossing (ZC) method. The anode pulse as a start signal taken by constant fraction discriminator (CFD) and a stop signal using ZC of a bipolar-shaped pulse. The time difference registered by a time-to-amplitude converter (TAC). It is well known that various charged particles produce scintillations with different decay constants, depending on their mass and charge, which results in

differences in ZC time. The large differences in amplitudes of the slow component decay time are crucial for separation of fast neutrons from γ-rays. The estimation of the number of photoelectrons per energy unit (phe/MeV) will be done by using the Compton edge of γ-rays from a 137 Cs source and a single photoelectron spectrum from the PMT. The response of the composite scintillators to fast neutrons measured by means of a neutron source. The detector shielded by 10cm of lead to reduce the intensity of high-energy γ-rays from the neutron source and 3 mm of copper to reduce the X-rays from lead. In conclusion, it is expected that the new material has a scintillation property in addition to use fascinating molecular characteristics, compact, light and environmental-friendly novel devices can be supplied at reasonable costs.

17-

Radiation protection program in Nuclear Fuel Fabrication Plant *(P6)*

Hade Elsayed

Egyptian Atomic Energy Authority, Cairo, Egypt

Radiation protection methodologies concerning individual monitoring, workplace monitoring and environmental monitoring in nuclear fuel fabrication facilities have been developed and applied to facilities in the Nuclear Fuel Manufacturing Pilot Plant (FMPP) of Egyptian Atomic Energy Authority (EAEA). External exposure to gamma, beta ray and neutron and internal exposure to alpha emitter are important issues for radiation protection at these facilities. Monitoring of airborne and surface contamination by alpha and beta/gamma emitters at workplace is also essential to avoid internal exposure. A criticality accident alarm system developed by FMPP has been proved through application at the

facilities for a long time. Air, solid and liquid effluents from facilities are monitored by continuous monitors or sampling methods to comply with regulations. Effluent monitoring has been carried out from the commissioning FMPP up to now to assess the radiological impacts on the public and the environment due to facility operation. In this paper we will be show the procedures the radiation protection program in the FMPP to protect the workers and the environment from the hazards of radiation.

18-

Impacts of climatic changes on natural hazards and radiocontaminants dispersion around nuclear instillations & and adaption strategy *(O12)*

Mostafa Sadek

Nuclear and Radiological Safety Research Center, EAEA, Cairo, Egypt

(Abstract not available)

19-

Utilizations of Egypt Second Research Reactor: current status and future directions *(O13)*

Mohamed Soliman

Egypt Second Research Reactor, Egyptian Atomic Energy Authority, Cairo, Egypt

Egypt Second Research Reactor (ETRR-2) is a multipurpose reactor with a nominal thermal power of 22 MW. The reactor is owned and operated by Egyptian Atomic Energy Authority. It has a various active utilizations including neutron activation analysis, neutron radiography, nuclear transformation doping, production of radioisotopes (tracers, medical and

industrial), and gem stones coloration. In addition, ETRR-2 supports the national goal for building the human capacity in the area of nuclear sciences and applications. It is planned to extend the scope of ETRR-2 utilizations through the installation of new facilities like neutron diffractometer and prompt gamma neutron activation coupled with imaging facility.
The presentation will explore the following topics:

1- Brief description of ETRR-2 and its facilities
2- Current experiments performed at neutron activation laboratory, neutron radiography facility, and radiotracers production for basic and applied sciences.
3- Radioisotopes production
4- Gem stone coloration
5- Planned experiments which include:
   i. Installing a sub-cadmium irradiation facility outside the core of ETRR-2 in order to perform epithermal neutron activation analysis.
   ii. Feasibility study for installation of prompt gamma activation analysis.
   iii. Designing and installing a loop irradiation facility for analysis of circulating liquid samples. It requires insertion of irradiation tube close to the reactor core.

20-

Assessment of the ability of reinforced concrete buildings for attenuation of Gamma ray emitted from a lost radiation source *(P7)*

Mohamed Abd El Monem Zaki Farahat
Radiation Control Division, Nuclear and Radiological Safety Research Center, Egyptian Atomic Energy Authority, Cairo, Egypt

The paper studies the ability of the reinforced concrete buildings to protect people from gamma ray hazards emitted from a lost radiation source and calculate the required safe distance to protect them. For this purpose, a proposed factory building has been studied which consists of a basement, a ground floor and two typical floors constructed of silty brick walls, reinforced concrete walls and reinforced concrete slabs. A gamma ray source ^{192}Ir (20 Ci) was used as a lost source. MCNP 5 code based on Monte Carlo technique was used to calculate the gamma doses rate that may reach to the people inside this building. Three cases were evaluated for the distance between the source and the building wall respectively 3 m, 10 m and 20 m. The doses rate has been estimated by ﷺsv/h for the three cases at different heights from the sidewalk level (radioactive source level). The dose rate had been calculated in the basement level - 0.30 m, at the sidewalk level 0.00 m, at the ground floor level 2.95 m, at the first floor level 6.20 m and finally at the second floor level 9.45 m. The results indicate that all gamma doses decrease with increasing the distance between the source and the measuring point. All Gamma doses decrease with increasing the height of measuring point from the source level (sidewalk level) at the same case. The safe floors which can protect the people from the dangerous effects of gamma ray emitted from a lost radiation γ-source ^{192}Ir (20 Ci) is ≥ 2.95 m from the radioactive source level. The obtained gamma dose results of MCNP 5 code are consistent with the obtained results of the manual calculation formula. So, this code is suitable for accurate calculations of gamma doses.

21-

Cross-section evaluation of the therapeutic radionuclide ^{103}Pd: Different production routes using commercial cyclotrons *(O14)*

B.M. Ali

Cyclotron Facility ,Experimental Nuclear Physics Department, Nuclear Research Centre, Egyptian Atomic Energy Authority, Cairo 13759, Egypt.

^{103}Pd radionuclides are widely used in internal radiotherapy, especially in the treatment of prostate cancer. We evaluated the proton and deuteron-induced reactions on rhodium ^{103}Rh(p,n)^{103}Pd and ^{103}Rh(d,2n)^{103}Pd. Nuclear model calculations were performed using the EMPIRE 3.2.3 code to validate the experimental literature data. The application of these data, particularly in calculating integrated yields, was discussed. The examined methods were compared in terms of practical application to produce ^{103}Pd.

22-

Semi empirical formula for (n,d) reaction cross-section at 14-15 MeV *(O15)*

Samra Nehaoua, Asma Ghezal, Fouzia Bouchelaghem, Nouri Benaidja

University of Msila, University pole, Bordj Bou Arreridj, M'sila 28000, Algeria

A semi empirical formula for (n,d) nuclear reaction cross section is proposed. The systematic was derived using analytical expressions for the calculation of the deuterium emission spectrum in nuclear reactions. The pre-equilibrium exciton model and the evaporation model are used to describe the deuterium emission. The experimental data are used to adjust free parameters in systematic formula at 14-15 MeV.

The systematics gives closer results to experimental data compared with formulas proposed earlier.

23-

Quasi-elastic correction in ^{4}He - ^{4}He elastic interactions at P_L= 4.32, 5.07 GeV/c *(O16)*

Ahmed M. Mosallem

Mathematics and Theoretical Physics Dept., NRC, Egyptian Atomic Energy Authority, Cairo, Egypt.

The ^{4}He - ^{4}He elastic scattering at P_L of 4.23 and 5.07 GeV/c is analyzed in the framework of the Glauber theory. The differential cross section evaluated using full Glauber graphs. The quasi-elastic scattering differential cross section calculated using Mont Carlo method was calculated. 4% of quasi-elastic differential cross section to the elastic one allows one to reproduce the experimental data quite well.

24-

Verification of uranium composite materials using active interrogation techniques for safeguards purposes *(O17)*

M. Tohamy

Experimental Nuclear Physics Department, Nuclear Research Center, Egyptian Atomic Energy Authority, Cairo 13759, Egypt

Uranium isotopic charecterization serving nuclear safegurds and security was done using both passive and active non-destructive techniques. The interrogated samples were natural uranium (NU), low-enriched uranium (LEU), and depleted uranium (DU) all in the form of uranium dioxide. The obtained spectra using both techniques were accumulated using a high-efficiency HPGe detector. Improving detector efficiency was developed using neural network (NN) method based on the obtained intrincic calibration data. The obtained enrichment

results of passive measurments showed good agreement with certified samples to within 1.12% in the case of LEU, 1.03% in the case of NU, and 1.04% in the case of DU.

Active interrogation was done using the neutron spectrum of a 5 Ci ^{241}Am-Be neutron source. Seven short-lived fission products (^{101}Tc, ^{97}Nb, ^{105}Ru, ^{92}Y, ^{91}Sr, ^{92}Sr, and ^{88}Kr) were chosen as indicators to provide a complete characterization of isotopic mass determination, uranium content, and enrichment. Isotopic masses of the samples were calculated using thermal and fast interrogations. Comparison of the obtained results of ^{238}U mass was found to agree within 0.2% based on fast interrogation, and within 0.3% of ^{235}U mass based on thermal interrogation.

Keywords: Non-destructive assessment, interrogation samples: NU, LEU & DU, thermal neutron induced-fission, fast neutron induced-fission, fission product indicators, ^{241}Am-Be source.

NUPPAC' 24

Notes

NUPPAC' 24
Notes

المؤتمر الثالث عشر للفيزياء النووية والجسيمية

NUPPAC' 24

كتاب الملخصات

26–23 سبتمبر 2024

مرسى مطروح، جمهورية مصر العربية